

# Application of Ultra-High-Speed Protection and Traveling-Wave Fault Locating on a Hybrid Line

Sthitaprajnyan Sharma, Amol Kathe, Titiksha Joshi, and Thamizhcholai Kanagasabai  
*Schweitzer Engineering Laboratories, Inc.*

Presented at the  
46th Annual Western Protective Relay Conference  
Spokane, Washington  
October 22–24, 2019

# Application of Ultra-High-Speed Protection and Traveling-Wave Fault Locating on a Hybrid Line

Sthitaprajnyan Sharma, Amol Kathe, Titiksha Joshi, and Thamizhcholai Kanagasabai,  
*Schweitzer Engineering Laboratories, Inc.*

**Abstract**—In this paper, we share a pilot installation experience of using ultra-high-speed (UHS) protection and traveling-wave fault locating (TWFL) on a hybrid line at a power utility in India. The 220 kV, 89 km hybrid line has two overhead line sections and an underground cable section in the middle. We selected this line, which is between a generating station and a substation, to evaluate the performance of the UHS protection and TWFL functions. It is one of two key lines supplying power to a metropolitan city and runs through thick forest as well as residential areas. The need for accurate fault locating and an adaptive autoreclosing scheme to block autoreclosing for faults on the underground cable section led to this project. The relays with UHS and TWFL functions are installed at the two terminals of the line and are connected via a direct fiber-optic communication channel. This paper elaborates on the following with field events:

- Energization of the hybrid line and configuration of the UHS protection and TWFL function.
- UHS protection performance for internal and external faults.
- TWFL performance for an internal fault.
- Monitoring of transient events to improve line maintenance.

## I. INTRODUCTION

Locating faults on hybrid lines with conventional fault-locating methods can be challenging. For hybrid lines, accurate fault locating is extremely important, and it may be deemed critical if the line runs through difficult terrain.

A major power utility in a metropolitan city in India operates a double circuit 220 kV, 89.35 km, three-section hybrid line between a generating station (S) and receiving station (R). The installed generating capacity of the generating station is 750 MVA ( $3 \times 250$  MVA). Each hybrid line has two overhead line sections with an underground cable section between them. The line passes over several roads, railways, and distribution lines and under extra-high-voltage (EHV) lines.

The existing protective relays with impedance-based fault locating have not been very effective in the hybrid line application. Existing protection includes a line current differential scheme as the primary protection, a distance element as the secondary protection, and directional overcurrent and earth-fault protection for backup protection.

The utility wanted to accurately locate faults and explore the possibility of only allowing autoreclosing for faults on the overhead line sections and inhibiting autoreclosing for faults on the underground cable section. A pilot installation of line protective relays with ultra-high-speed (UHS) protection and traveling-wave fault-locating (TWFL) technology was

implemented on one of the hybrid lines. The utility wanted to learn about this new technology, gain experience, and evaluate the performance of the relays on their 220 kV system.

In this paper, Section II briefly discusses UHS protection principles and summarizes the procedure for applying a double-ended TWFL method on a hybrid line. Section III provides information about the selected pilot line and the utility's present protection practices for this line. Section IV presents details about the commissioning of the two UHS relays and the line energization test to configure the fault locator. Section V discusses the overall experience from the pilot installation and analyzes the performance of the UHS protection and TWFL technology for multiple faults recorded on the system. Because of high-resolution event recording, the UHS relays can capture transient events such as fault precursors (incipient faults) or indicate events such as breaker restrike, lightning strikes, failing electrical equipment, and other incidents [1]. Section V also discusses one specific incident where several transient events were captured prior to a fault on the system.

## II. OVERVIEW OF UHS PROTECTION AND FAULT LOCATING

This section briefly explains the concepts of UHS protection elements and double-ended TWFL on hybrid lines. It also discusses adaptive autoreclose control logic to inhibit reclosing for faults on underground cable sections [2].

### A. Incremental-Quantity-Based Protection

The time-domain (TD) UHS protective relays installed for this pilot project use voltage and current incremental quantities, which are the differences between a present instantaneous sample and a one-cycle old sample. The incremental quantities contain the pure fault voltage and current information and exclude any preload information [3]. These signals are filtered with a low-pass filter and are then applied to directional and distance elements. The relay calculates incremental voltage and incremental replica currents for six measurement loops.

#### 1) Directional Element: TD32

The TD32 element provides a fast, secure, and dependable directional indication. This element is used as part of a permissive overreaching transfer trip (POTT) scheme. The element calculates the operating torque as a product of sign-inverted incremental voltage and incremental replica current. It also calculates the forward and reverse restraining torques based on the incremental replica current and forward/reverse impedance thresholds.

For a forward fault, the incremental voltage and incremental replica current have opposite polarities, which results in a positive torque. For a reverse fault, the incremental voltage and incremental replica current have the same polarity, which results in a negative torque. The calculated torques are integrated and the operating torque is compared with the restraining torques. References [3] and [4] discuss the directional element logic in detail.

### 2) *Underreaching Zone 1 Distance Element: TD21*

The TD21 element is a fast underreaching distance element used for instantaneous tripping. This element calculates the incremental voltage change at the reach point and compares it with the pre-fault voltage at the same reach point. For an in-zone fault within the reach point, the calculated incremental voltage change at the reach point will be greater than the pre-fault reach point voltage. For a fault beyond the reach point, the calculated incremental voltage change at the reach point will be less than the pre-fault reach point voltage [3].

In Section V, we analyze the operation of TD32 and TD21 for internal and external faults on the pilot installation.

### B. *Traveling-Wave (TW) Based Protection*

The pilot UHS protective relay includes a TW-based directional element (TW32) and a TW-based differential protection scheme (TW87). References [4] and [5] discuss TW protection elements and their field performance in detail. We do not investigate TW32 and TW87 operation in detail in this paper. The following points summarize the nature of current and voltage TWs for different fault conditions and aid in basic TW analysis:

- The polarities of the first voltage and current TWs indicate the fault direction. For a forward fault, the voltage TW and current TW have opposite polarities; for a reverse fault, the voltage TW and current TW have the same polarity. This fundamental principle forms the basis of TW32 logic.
- For an internal fault, the first current TWs detected at the local and remote line terminals have the same polarity and should be separated by less than the TW line propagation time. For an external fault, the first current TWs detected by the local and remote line terminals have opposite polarities and should be separated by the TW line propagation time. This fundamental principle forms the basis of TW87 logic.
- A fault on a parallel line results in same-polarity current TWs being detected at the protected line terminals. The TW87 scheme applies additional security for external faults on a parallel line. The scheme verifies whether the operating current TW (IOP) polarity is consistent with the pre-fault voltage (VPOL) at the fault location. For an internal fault on the protected line, it is expected that the VPOL polarity will match the IOP polarity. This polarity pattern is reversed for faults on a parallel line.

### C. *Fault Locating on Hybrid Lines*

The pilot UHS protective relay provides fault location information based on two methods: impedance-based and TW-based. Impedance-based fault-locating methods do not provide high-accuracy results when applied to a hybrid line with overhead line and underground cable sections. References [2] and [6] summarize the general challenges, accuracy-limiting factors, and the specific hybrid line challenges of impedance-based fault-locating methods.

In hybrid line applications, the main challenges include line nonhomogeneity and different line impedance data for overhead line and underground cable sections. The double-ended TWFL method overcomes these challenges. This paper refers to the double-ended TWFL principle and discusses extending this principle to hybrid line applications and leveraging TW fault location information to adaptively control autoreclose logic.

#### 1) *The Double-Ended TWFL Method for a Two-Terminal Homogeneous Line*

Faults on transmission lines launch voltage and current TWs that propagate from the fault point to line terminals. The fault locator embedded in the UHS relay uses this TW information and employs two methods to determine the fault location: double-ended based and single-ended based. As the name indicates, the double-ended method works by using data obtained from both ends of the line. It requires a communication channel to exchange TW arrival time information and provide synchronization between the two UHS relays to align the data. A direct fiber-optic channel is one of the ways to achieve this. Another option is to use a global positioning system (GPS) clock at both line terminals to ensure time synchronization and send the TW arrival time information to a central system. The central system can use this information to compute the fault location offline.

Consider a fault at a distance of  $M$  mi or km from Terminal S and at a distance of  $LL - M$  mi or km from Terminal R. Equation (1) from [2] shows the double-ended TW-based fault location calculation. It includes the first TW arrival times from both line terminals, total line length, and TW line propagation time for the entire line length.

$$M = \frac{LL}{2} \cdot \left( 1 + \frac{t_S - t_R}{TWLPT} \right) \quad (1)$$

where:

$M$  is the double-ended TW-based fault location in mi or km.

$LL$  is the total line length in mi or km.

$TWLPT$  is the TW line propagation time.

$t_S$  is the first TW arrival time at Terminal S.

$t_R$  is the first TW arrival time at Terminal R.

Equation (1) can be modified to compensate for current transformer (CT) cable delays at the two terminals. The CT cable delay compensation (TWCPT) is a user setting and is accounted for in the fault location calculation shown in (2).

$$M = \frac{LL}{2} \cdot \left( 1 + \frac{(t_S - TWCPT_S) - (t_R - TWCPT_R)}{TWLPT} \right) \quad (2)$$

The double-ended TWFL method is simple. Unlike the single-ended method, it only requires identification of the first TWs. The double-ended method is field-proven and provides accurate results within a range of one tower span, on average. The single-ended method uses the TW data from one end of the line and must consider the first TW, as well as several successive TWs, reflected from the fault and other terminations in the system [7]. In the case of a hybrid line, the single-ended method is challenging due to the reflections from every section termination on the line, and therefore it is not discussed in this paper.

### 2) Applying the Double-Ended TWFL Method to Hybrid Lines

Equation (1) provides a fault location calculation for a two-terminal homogeneous line. The TW propagation velocity (PV) can be calculated as shown in (3).

$$PV = \frac{LL}{TWLPT} \quad (3)$$

In the case of a two-terminal hybrid line, the TW propagation velocity in the overhead line is different than in the underground cable. As a result, (1) must be corrected to account for these differences in the TW propagation velocities among different sections of a hybrid line. For example, the TW propagation velocity in an overhead line can be approximately 98 percent of the speed of light, while in an underground cable section it can be approximately 55 percent of the speed of light.

Consider a nonhomogeneous hybrid line with two overhead line sections and one underground cable section in the middle. The overhead line sections have lengths  $LL_1$  and  $LL_3$  and TW propagation times of  $TWLPT_1$  and  $TWLPT_3$ , respectively. The underground cable section has a length of  $LL_2$  and TW propagation time of  $TWLPT_2$ . The total line length ( $LL$ ) and TW propagation time ( $TWLPT$ ) can be calculated in (4):

$$\begin{aligned} LL &= LL_1 + LL_2 + LL_3 \\ TWLPT &= TWLPT_1 + TWLPT_2 + TWLPT_3 \end{aligned} \quad (4)$$

Reference [2] summarizes fault locating on a hybrid line in the following three steps:

1. Calculate fault location  $M^*$  assuming a homogeneous line and substituting total line length ( $LL$ ) and propagation time ( $TWLPT$ ) in (1).
2. Calculate the time  $t^*$  assuming a homogeneous line represented by a straight-line characteristic.
3. Calculate the actual fault location  $M$  by projecting the calculated time  $t^*$  onto the actual nonhomogeneous hybrid line characteristic.

Fig. 1 shows an example where the fault location ( $M^*$ ), calculated using (1), suggests that the fault is on an overhead line (OHL) section. By applying the previously mentioned correction method, the actual fault location ( $M$ ) can be calculated, and the fault appears to be on the underground cable (UGC) section. This is important information that could be used for the application described in the next section (Section D).

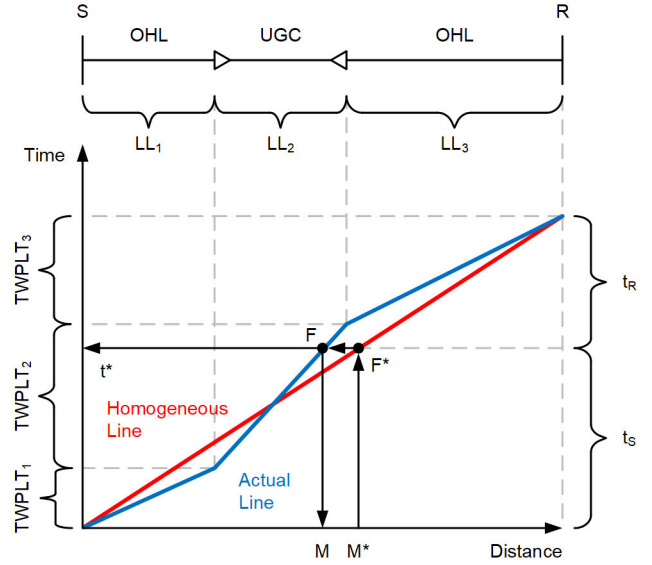


Fig. 1. Illustration of a three-step method to calculate double-ended TW fault location for a nonhomogeneous line [2]

### 3) Measuring TW Line Propagation Time

To configure a TW-based fault locator and achieve better fault-locating accuracy, it is essential to accurately determine the TW propagation time for every section of the hybrid line. This can be achieved by a line energization test during relay commissioning. The idea is to energize the line from the local terminal while the remote circuit breaker is open. The expected sequence of events is summarized as follows:

1. As the line is energized and the circuit breaker closes at the local line terminal, a voltage step change is applied that launches a transient. The incident voltage and current TWs travel forward to the remote end of the line.
2. The characteristic impedances of overhead lines (approximately 300–400  $\Omega$ ) and underground cables (approximately 30–80  $\Omega$ ) are very different [8]. As a result, every transition point between an overhead line and underground cable acts as a termination at which a part of the incident TW reflects and a part of it is transmitted. The reflected TW travels back to the energized terminal and the transmitted TW travels forward to the remote line terminal.
3. At the remote line terminal, since the circuit breaker is open, the incident current TW completely reflects with an opposite polarity.

As a result, the TW travels the total line length twice: forward when it is launched and back to the energizing terminal after reflection from the remote end.

References [8] and [9] explain the concepts of TW reflection and transmission coefficients. These coefficients help in determining the magnitude and polarity of reflected and transmitted waves. In general, current TWs reflected from an overhead line to an underground cable transition have the same polarity as the incident wave, while current TWs reflected from

an underground cable to an overhead line transition have the opposite polarity as the incident wave. This information can aid in identifying the correct reflected wave when measuring the TW line propagation time. Reference [2] provides numerical examples to calculate the incident, transmitted, and reflected TWs for a line energization test and faults on different sections of a hybrid line.

#### D. Adaptive Autoreclosing Control Logic on Hybrid Lines

The double-ended TW fault location information is used by the adaptive autoreclosing control logic to 1) selectively allow single-pole tripping and reclosing for faults on overhead line sections and 2) force three-pole tripping and block autoreclosing for faults on underground cable sections of a hybrid line. We can configure multiple blocking regions in this application. If the calculated double-ended TW fault location falls within any of the specified blocking regions, the logic asserts an autoreclosing cancel control digital bit (ARC). This digital bit asserts within a few milliseconds after the fault and can be configured to control the tripping logic and autoreclosing scheme. If the fault location information is missing, such as for a communication failure, the logic allows or blocks reclosing based on user-selected default settings. The adaptive autoreclosing control logic is shown in Fig. 2.

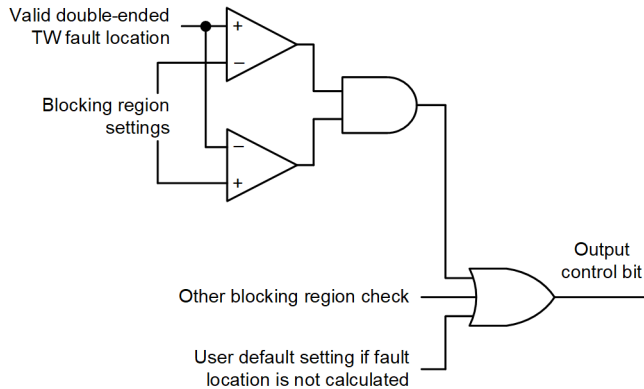


Fig. 2. Adaptive autoreclosing control logic diagram

### III. PILOT INSTALLATION

#### A. Pilot Line Configuration

The power generated at Station S is transferred via the 220 kV double circuit hybrid line and supplied to Station R, as shown in Fig. 3. At peak load conditions, the power transferred by these two lines may reach 700 MVA or greater, and both lines are equally critical to the utility. According to the utility, they have about five to seven faults per year on each circuit. Most of these faults are on the overhead line sections and commonly occur during the monsoon season.

The two hybrid lines are configured identically. They are on double circuit towers for a major part of the line length, except where they separately pass under EHV lines on single circuit towers. Single-core cross-linked polyethylene (XLPE) cables are used for each phase in the underground cable section of the 220 kV lines. For the pilot project, protective relays with UHS protection and TWFL functionality were installed at both terminals of one of these hybrid lines. A direct fiber-optic communication channel is available between Stations S and R, which runs along the ground wire in the overhead line sections and is buried underground along with the underground cable section.

#### B. Existing Protection Philosophy

The utility presently uses a line current differential scheme via a direct fiber-optic communication channel as primary protection and a conventional phasor-based distance protection with a permissive underreaching transfer trip (PUTT) scheme as secondary protection. Directional overcurrent and earth-fault protection elements provide backup protection. The existing protection scheme treats the hybrid line as a two-terminal homogeneous line. The existing protective relays employ an impedance-based fault-locating method using the total line impedance value of the hybrid line, which is the sum of the impedances of the overhead line and underground cable sections. This impedance-based fault-locating method does not provide a highly accurate fault location because of the challenges specific to cables and hybrid lines. This is one of the major challenges the utility faces with their existing scheme.

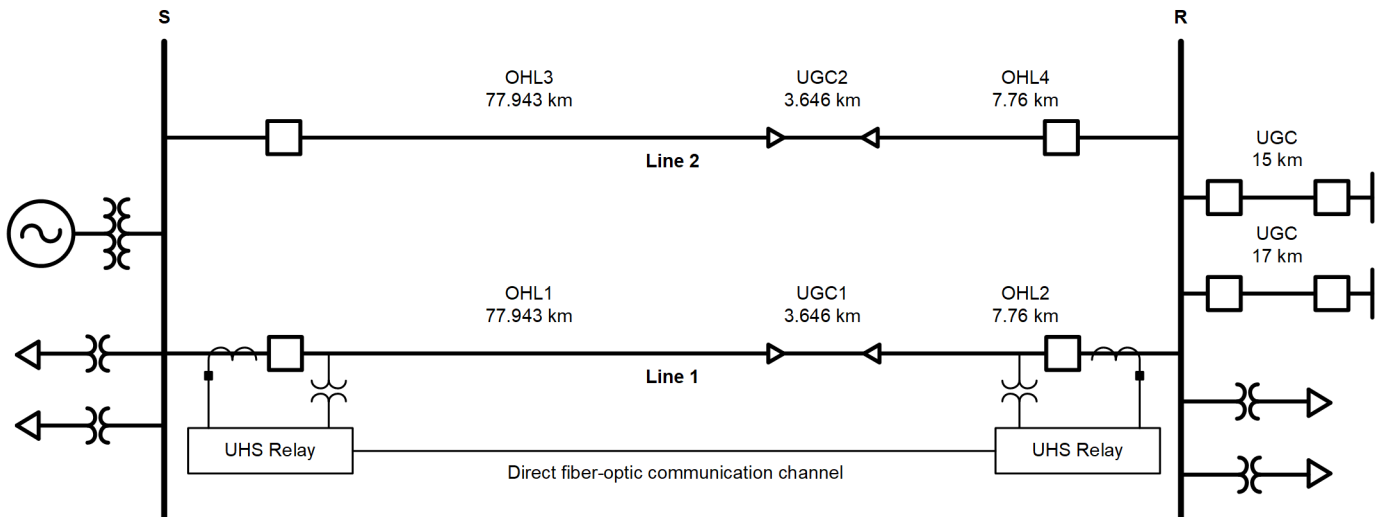


Fig. 3. System one-line diagram

Autoreclosing is also in service in the existing scheme. The line current differential trip initiates autoreclosing in the distance relay. The distance relay must first identify a fault as a single-phase-to-ground fault within Zone 1 and issue a single-pole trip in order to release a single-shot autoreclose command. The distance relay issues the autoreclose command after an open interval time of 400 ms.

For an evolving fault, a multiphase fault, or an unsuccessful autoreclose event, the existing scheme trips all three poles of the line breaker and locks out. The directional overcurrent backup protection issues a three-pole trip when a fault is detected. The present scheme is not selective and may generate an autoreclose command even for a single-phase fault on the underground cable section, including faults at the termination of the underground cable. Reclosing for faults on an underground cable could lead to severe cable damage and expensive repairs. As a result, the utility wanted to explore the possibility of an adaptive autoreclosing scheme to block autoreclosing for faults in the underground cable section and cable terminations.

#### IV. COMMISSIONING

Fig. 3 shows the system one-line diagram. The system data are provided in Table I.

TABLE I  
SYSTEM DATA

System Parameter	System Data
Overhead line positive-sequence impedance	$0.07348 + 0.3938j \Omega/\text{km}$
Overhead line zero-sequence impedance	$0.2991 + 1.112j \Omega/\text{km}$
Underground cable positive-sequence impedance	$0.0318 + 0.13j \Omega/\text{km}$
Underground cable zero-sequence impedance	$0.12 + 0.08j \Omega/\text{km}$
CT ratio (Terminal S)	1000
CT nominal secondary current (Terminal S)	1 A
PT ratio (Terminal S)	2000
CT ratio (Terminal R)	1000
CT nominal secondary current (Terminal R)	1 A
PT ratio (Terminal R)	2000
Total line length	89.35 km

The UHS relays with TWFL functionality are installed at both terminals of Line 1. The relays are connected via a direct fiber-optic communication channel, and Terminal R is connected to a GPS clock for absolute time reference.

##### A. Communications

A direct fiber-optic communication channel was available between Terminals S and R. This channel was used in the pilot installation to exchange current and voltage signals and TW arrival time information between the two relays. Prior to commissioning, the link-loss budget of the communication channel and selection of suitable fiber-optic small form-factor

pluggable (SFP) transceivers were verified with the help of the telecommunications department of the utility. The UHS relay monitors the communication channel in real time and provides valuable information, such as channel status, link delay, and SFP transceiver transmit and receive power. This information was used to ensure that the communication channel was in a healthy state.

The high-accuracy GPS clock was only available at Terminal R. The protection scheme involving two UHS relays with a healthy direct fiber-optic communication channel does not require absolute time from an external time source. The high-accuracy timekeeping in the UHS relays ensures synchronization between relays, and both relays remain synchronized to each other, regardless of external time source availability. This synchronization provides the necessary data alignment between the relays at Terminals S and R. The GPS clock at Terminal R only provides an absolute time reference for post-event analysis.

##### B. Line Energization Test

During commissioning, a line energization test was performed from both ends of the line to measure the TW propagation time for each section of the hybrid line. The line was first energized from Terminal S, with the Terminal R circuit breaker open; the test was then repeated by energizing Terminal R, with the Terminal S circuit breaker open.

###### 1) Energization From Terminal S With Terminal R Open

Fig. 4 shows the currents and voltages captured during line energization from Terminal S. These raw current and voltage signals were captured at a 1 MHz sampling rate.

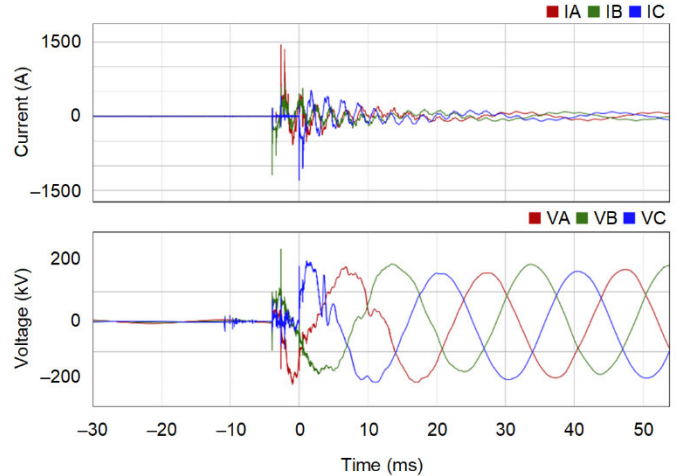


Fig. 4. Raw currents and voltages captured during line energization from Terminal S

The TW information is extracted by passing the raw signals through a differentiator smoother filter [9]. Traveling waves contain two modes: aerial (alpha and beta) and ground [9]. The ground mode exhibits larger attenuation and dispersion. Typically, it is best to select the alpha aerial mode corresponding to the last circuit breaker pole that closed. Fig. 5 shows the current TWs recorded at Terminal S.

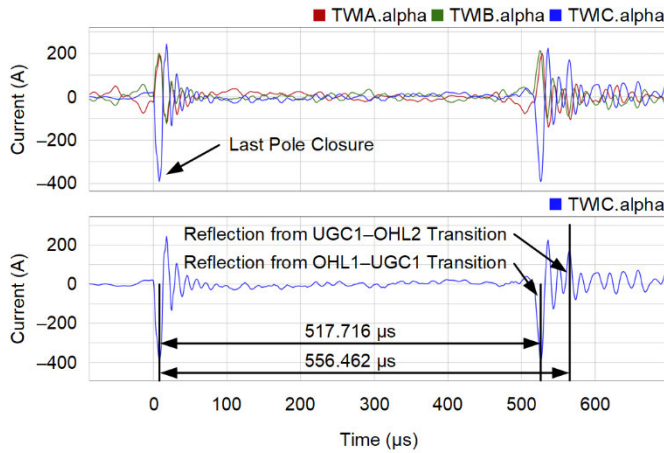


Fig. 5. Current TWs captured during line energization from Terminal S

Observing the alpha aerial current referenced to Phase C, Terminal S first detects the reflection from the OHL1-UGC1 transition at 517.716  $\mu\text{s}$ , followed by a reflection from the UGC1-OHL2 transition at 556.462  $\mu\text{s}$ . Note that this is the roundtrip time because the TW launched from energizing Terminal S travels forward toward the open remote line terminal, reflects from every transition point between the overhead line and underground cable along the line, and travels back to the energizing Terminal S. The TW propagation time for any section can be calculated by first determining the section roundtrip time from available measurements and then dividing these calculated values by 2. Table II shows the TW line propagation times calculated for sections OHL1 and UGC1.

TABLE II  
TW PROPAGATION TIME MEASUREMENTS

Section	Roundtrip Time	TWLPT
OHL1	517.716 $\mu\text{s}$	258.858 $\mu\text{s}$
UGC1	556.462 – 517.716 = 38.746 $\mu\text{s}$	19.373 $\mu\text{s}$

During the test, it was difficult to identify the reflection from remote Terminal R and determine the TW propagation time for section OHL2. One of the reasons for this is TW attenuation and dispersion [8] [9]. As the TWs travel longer distances and pass through overhead lines and cables, they attenuate and exhibit a dispersion pattern. Underground cables exhibit much higher dispersion and attenuation than overhead lines. In addition to these effects, any transition between an overhead line and underground cable section results in reflection and reduction in the transmitted TW signal level that reaches the remote line terminal. As the TW signal reaches the remote line terminal, it may be reduced even more if there are other TW signals arriving at that terminal from different paths at the same time. For these reasons, it is possible that the energizing terminal may not detect reflections from the remote end of the line or from transition points that are far away from the energizing terminal. Therefore, it is a good practice to perform line energization tests from both ends of the line.

## 2) Energization From Terminal R With Terminal S Open

The previously described line energization test was repeated by energizing Terminal R, with the Terminal S circuit breaker open. Fig. 6 shows the raw current and voltage signals captured every microsecond at Terminal R.

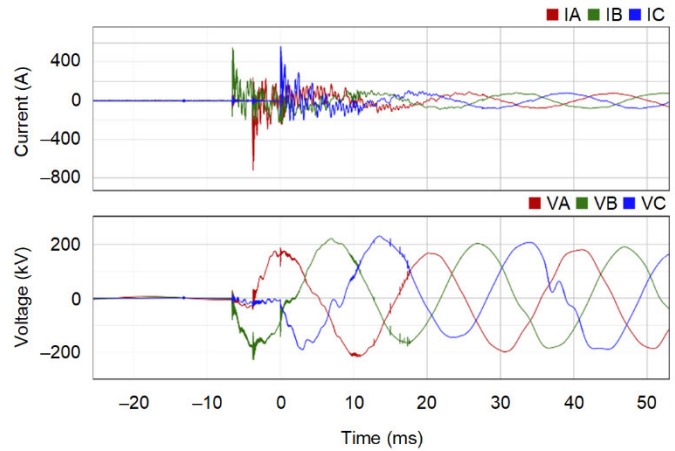


Fig. 6. Raw currents and voltages captured during line energization from Terminal R

Fig. 7 shows the current TWs recorded at Terminal R. Since Pole C was the last to close, the alpha aerial mode referenced to Phase C was used to measure the roundtrip time.

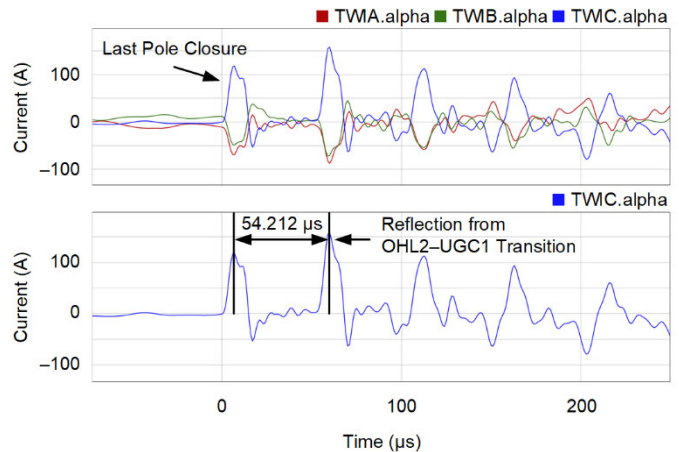


Fig. 7. Current TWs captured during line energization from Terminal R

During this test, the reflection from the OHL2-UGC1 transition was identified, and the roundtrip time measurement was used to calculate the TW propagation time for section OHL2, as shown in Table III.

TABLE III  
TW PROPAGATION TIME MEASUREMENT

Section	Roundtrip Time	TWLPT
OHL2	54.212 $\mu\text{s}$	27.106 $\mu\text{s}$

Table IV summarizes the line length and TW propagation time data for the pilot hybrid line.

TABLE IV  
PILOT HYBRID LINE TW DATA

Section	Line Length	TWLPT
OHL1	77.943 km	258.858 $\mu$ s
UGC1	3.646 km	19.373 $\mu$ s
OHL2	7.76 km	27.106 $\mu$ s
Total	89.349 km	305.337 $\mu$ s

### C. Relay Settings

Because of a lack of data available during commissioning and this being a pilot installation, the TD32 forward impedance setting was set to a minimum value. The TD32 reverse impedance setting was set to 30 percent of the positive-sequence line impedance magnitude. The TD21 phase reach was set to 70 percent of the line, and the TD21 ground reach was set to 65 percent of the line.

The fault locator was configured using the line length and TW line propagation time data provided in Table IV. The adaptive autoreclosing control logic was configured by setting the blocking region equal to the length of the underground cable section, plus a security margin of 600 m to avoid spurious reclosing on cable faults. In cases where the fault location information was unavailable, the default setting was set to cancel the autoreclosing. The utility wanted to understand and evaluate the performance of the UHS relays before wiring them to trip the line circuit breakers. As a result, the relay outputs were not used to trip the line circuit breaker and control the existing autorecloser scheme.

## V. FIELD EVENT ANALYSIS

This section focuses on the performance of the protection elements and fault locator for different fault events that occurred on the pilot system throughout the year following commissioning.

### A. Internal Phase A-to-Ground Fault on September 24, 2018

This was the first internal fault on Line 1 reported by the utility after the UHS relays were commissioned. Fig. 8 and Fig. 9 show the current and voltage signals at Terminals S and R, respectively. Fig. 10 and Fig. 11 show that the incremental voltage and incremental replica current had opposite polarities during the fault. As a result, TD32FA and TD32F asserted in less than 1 ms, indicating a forward fault direction and Phase A as the faulted phase. The ground distance element outputs, TD21AG and TD21G, asserted in 6 to 7 ms at both terminals with correct faulted phase identification.

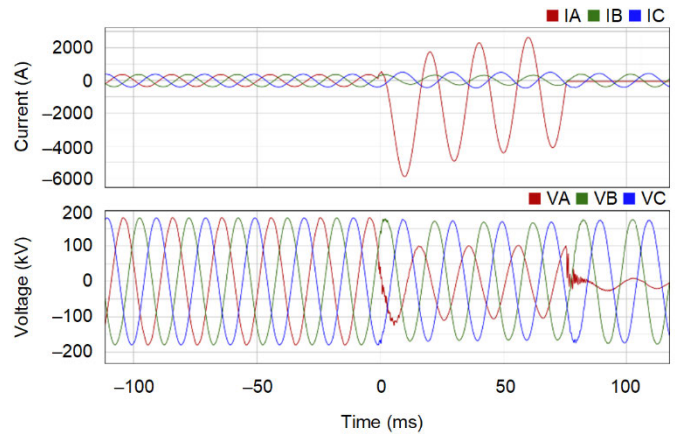


Fig. 8. Current and voltage signals for an internal Phase A-to-ground fault at Terminal S

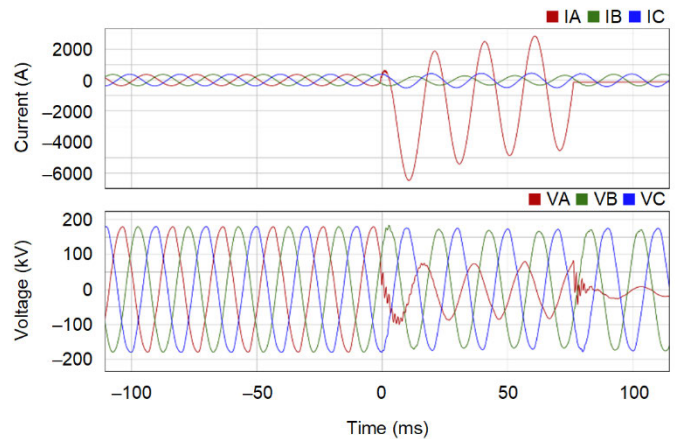


Fig. 9. Current and voltage signals for an internal Phase A-to-ground fault at Terminal R

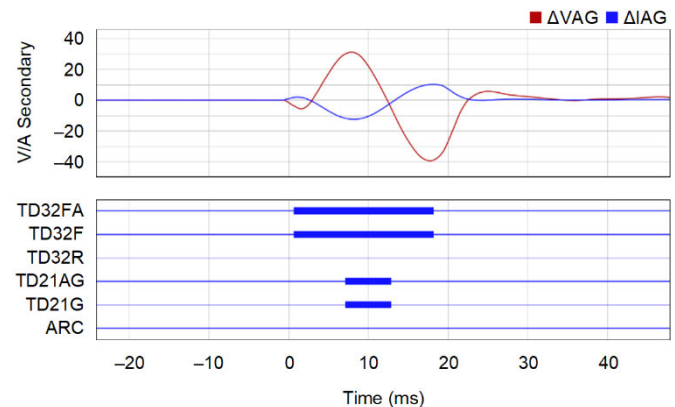


Fig. 10. Voltage and scaled current incremental quantities and TD32 and TD21 response for an internal Phase A-to-ground fault at Terminal S

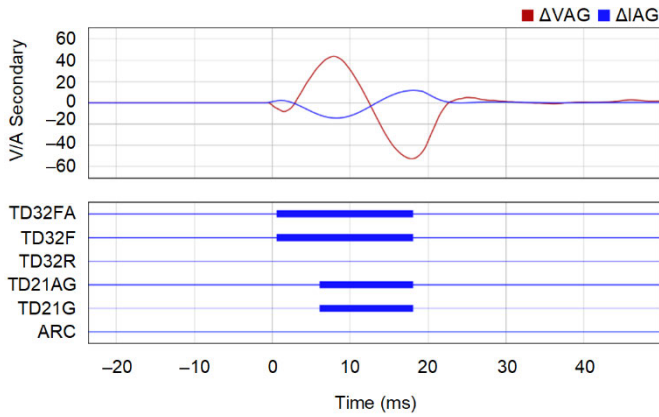


Fig. 11. Voltage and scaled current incremental quantities and TD32 and TD21 response for an internal Phase A-to-ground fault at Terminal R

Table V shows the TW double-ended fault location reported by the relays at Terminals S and R. The fault was on the overhead line section OHL1, and the autoreclosing control logic did not assert the autoreclose cancel output bit ARC at either terminal.

TABLE V  
TW FAULT LOCATION REPORTED BY THE UHS RELAY

Terminal	Fault-Locating Method	Fault Location
S	Double-ended TWFL	51.342 km
R	Double-ended TWFL	38.010 km

### B. Internal Phase A-to-Ground Fault on February 27, 2019

The utility reported an internal Phase A-to-ground fault on one of the overhead line sections of Line 1. Fig. 12 shows the current and voltage signals and protection performance at Terminal R. TD32FA and TD21AG correctly operated, indicating an in-zone forward Phase A-to-ground fault. The UHS relay issued a trip in less than 2 ms. Terminal R transmitted a permissive key signal (KEYA) to Terminal S when TD32F asserted.

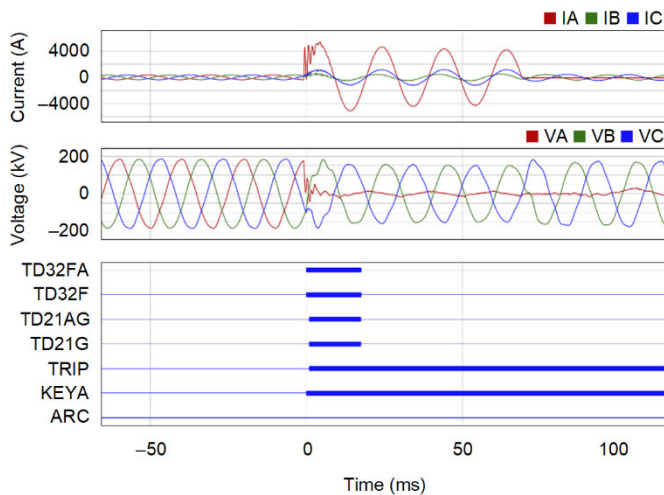


Fig. 12. Current and voltage signals and protection performance at Terminal R

Fig. 13 shows the first current and voltage TWs during the fault at Terminal R. Their polarities are opposite, indicating a forward fault.

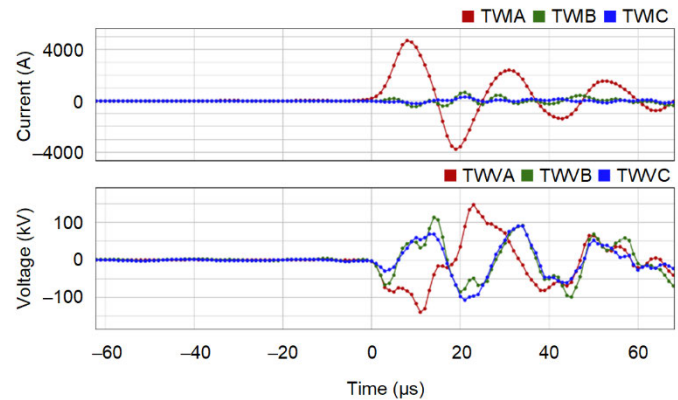


Fig. 13. First current and voltage TWs during an internal fault at Terminal R

Fig. 14 shows the current and voltage signals and protection performance at Terminal S. TD32FA operated, indicating a forward fault in Phase A, but TD21G did not operate because the fault was at 98 percent of the line and beyond the reach point setting. Terminal S operated on a POTT scheme over the direct fiber-optic channel after it received the permissive signal (PTRXA) and issued a trip in less than 2 ms.

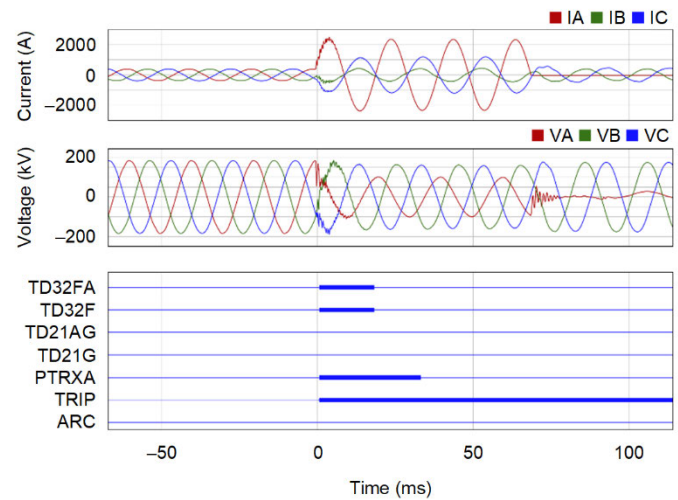


Fig. 14. Current and voltage signals and protection performance at Terminal S

Table VI shows the TW double-ended fault location reported by the relays at Terminals S and R. The fault was on the overhead line section OHL2, closer to Terminal R.

TABLE VI  
TW FAULT LOCATION REPORTED BY THE UHS RELAY

Terminal	Fault-Locating Method	Fault Location
S	Double-ended TWFL	87.649 km
R	Double-ended TWFL	1.702 km

Because this was a fault on the overhead line section, the autoreclosing control logic did not assert the output bit ARC, as shown in Fig. 12 and Fig. 14. The utility also confirmed that a successful line reclosing was initiated from an existing autorecloser scheme for this fault.

### C. External Phase A-to-Ground Fault on June 5, 2019

A Phase A-to-ground fault occurred on Line 2 (the parallel line not monitored by the UHS relays) on June 5, 2019 at 11:25 a.m., and the Line 2 relays initiated a trip for this fault. The UHS relays on Line 1 restrained correctly, with no operation of the TD21 elements and POTT scheme. Fig. 15 shows the current and voltage signals and protection response at Terminal S. TD32RA and TD32R operated, indicating a reverse fault in Phase A.

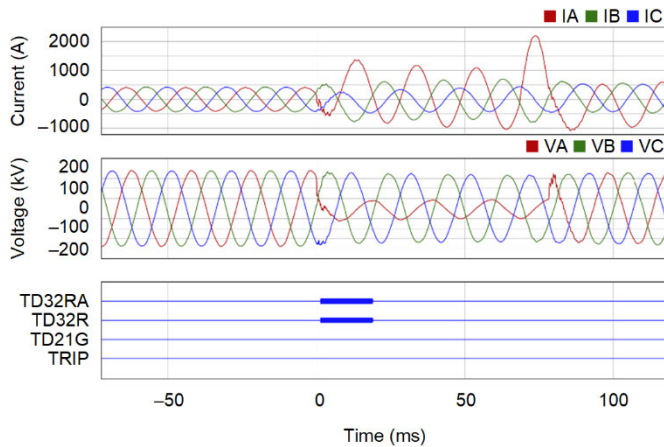


Fig. 15. Current and voltage signals and protection performance at Terminal S

Fig. 16 shows that the incremental voltage and incremental replica current had the same polarity for the reverse fault at Terminal S.

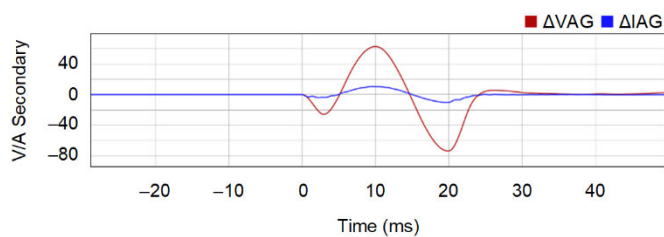


Fig. 16. Incremental voltage and scaled incremental replica current relationship for the reverse fault at Terminal S

Fig. 17 shows the current and voltage signals and protection response at Terminal R. TD32F operated and TD21G restrained because the fault was on the parallel line closer to Terminal S.

Fig. 18 shows that the first current and voltage TWs in Phase A at Terminal S have the highest magnitude among the three phases, and their polarities match. This is an indication of a reverse fault in Phase A.

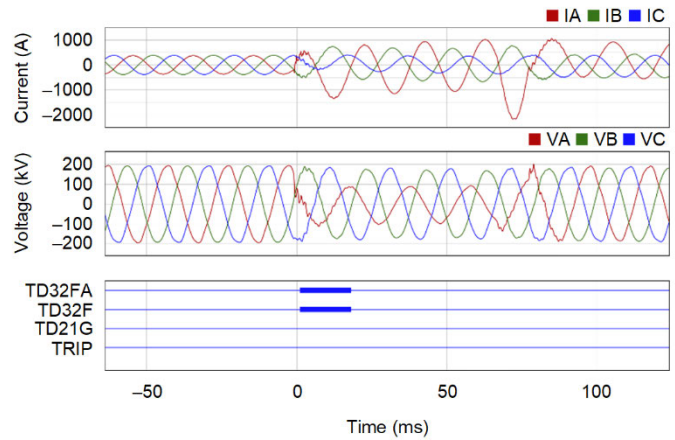


Fig. 17. Current and voltage signals and protection performance at Terminal R

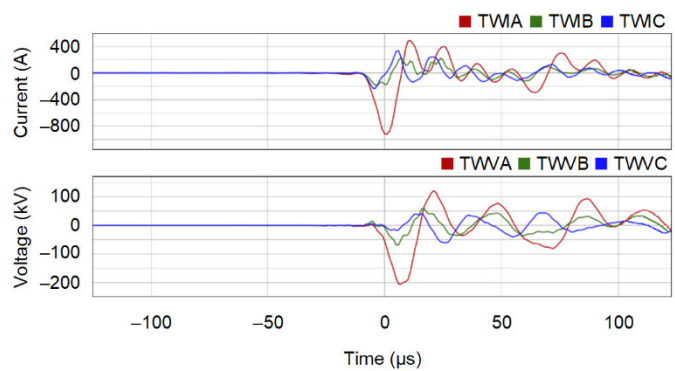


Fig. 18. Current and voltage TWs during an external fault at Terminal S

Because the very first TWs were successfully captured by the UHS relays for this fault, their arrival times can be used to calculate the fault location offline. Fig. 19 shows the first current TWs at Terminals S and R.

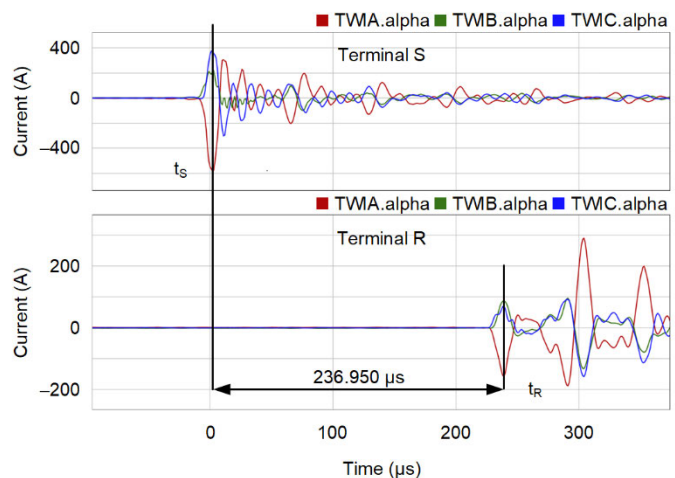


Fig. 19. First current TWs captured at Terminals S and R

Substituting  $t_s = 0 \mu\text{s}$  and  $t_r = 236.950 \mu\text{s}$  in (1), we obtain the fault location from Terminal S in (5).

$$M = \frac{89.35}{2} \cdot \left( 1 + \frac{-236.950}{305.34} \right) = 10.01 \text{ km} \quad (5)$$

The location of 10.01 km corresponds to  $t^* = 34.1950 \mu\text{s}$ , assuming a homogeneous line. The value of  $t^*$  using the hybrid line characteristic gives a true fault location of 10.25 km from Terminal S on Line 2. The existing distance relay at Terminal S reported an impedance-based fault location of 9.1 km.

As explained in Section II, the TW87 scheme includes a VPOL-IOP security check to determine whether the fault is internal or external, specifically for parallel lines. In this event, the fault occurred at a positive point on wave of the pre-fault voltage at the fault location (VPOL), and the operating current TW polarity (IOP) was negative. This offline analysis also confirmed that the fault was external and on the parallel line (Line 2).

Fig. 20 shows the voltage and current signals captured by the protective relay at Terminal S on Line 2. The event report shows the complete fault sequence: a Phase-A-to-ground fault resulted in opening a single pole, followed by an open interval time. After the open interval time expired, the line reclosed onto the fault, resulting in a three-pole trip and lockout.

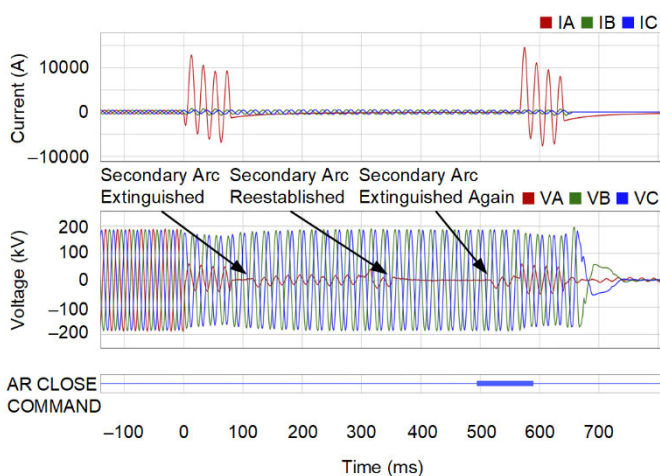


Fig. 20. Fault sequence captured by the protective relay at Terminal S on Line 2

The utility crew did not find any visual indication of a permanent fault following the lockout. A manual reclose was therefore attempted and the reclose was successful. It is interesting to note that the secondary arc extinguished and re-ignited during the open interval time. It is possible that the existing open interval time setting of 0.4 seconds was not adequate for the air to be deionized, thus resulting in the fault upon line reclose. The utility is evaluating the reasons for using a 0.4 second open interval time. Reference [10] provides an empirical formula shown in (6) to find an average open interval time for the fault arc to deionize and not restrike; this formula applies when all three phases are opened and there is no trapped energy, such as shunt reactors. For single-pole tripping applications, a longer open interval time is recommended.

$$t_{\text{open}} = \frac{\text{System Voltage}_{\text{kV}}}{34.5} + 10.5 \text{ cycles} \quad (6)$$

#### D. Monitoring Line Events Based on TWs

Prior to the fault on Line 2 at 11:25 a.m. on June 5, 2019, there were several transient events recorded by the UHS relays during a 30-minute interval. These transient events did not result in relay tripping operation and motivated the authors to perform offline analysis. For the offline analysis, the goals were to 1) identify if the events originated from the monitored line (Line 1), 2) calculate the location of the source of the transient event, and 3) report the event locations to the utility for field investigation. Fig. 21 provides an example of the transient signals captured at Terminal S at around 11:04 a.m.

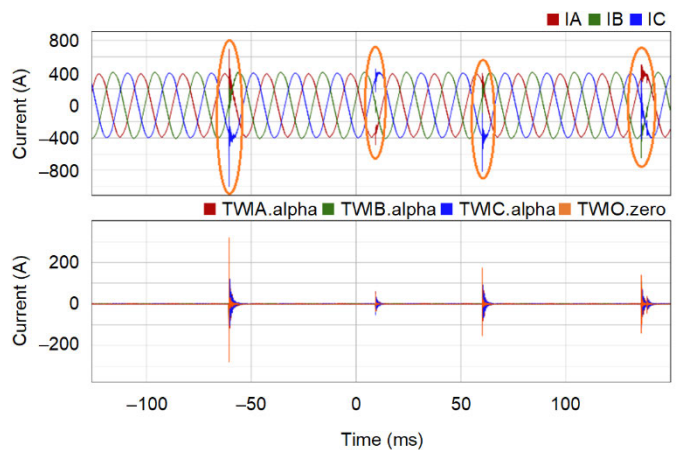


Fig. 21. An example of multiple transient events recorded at Terminal S (circled on the top graph)

The transient events generated significant TWs, and these were used to calculate the location of the transients by using the double-ended TWFL method. Fig. 22 shows the summary of these event locations calculated from Terminal S. On the x-axis, the line length is divided into bins of 0.25 km intervals, and the bin midpoint locations are marked as 0.25, 0.5, 0.75, and so on. Each bin has an event counter that increments if the calculated event location falls within the bin. Each event counter counts the internal and external events separately. It can be observed from Fig. 22 that several bins between 11 km and 27 km have a non-zero event count, and the event count in some of the bins is greater than one. An event count of greater than one indicates a recurring transient event and a trouble spot on the line that needs to be investigated by the field crew. A recurring event from the same location may also fall in adjacent bins, considering the smaller bin width and double-ended TWFL accuracy. As a result, three consecutive bins with an event count of one each is equally concerning and needs to be investigated. This event analysis was presented to the utility and they were requested to investigate the locations.

This section demonstrates that TWs can be used to identify trouble spots on the system. TWs may be detected before a fault occurs as fault precursors or during low-energy events such as partial discharge due to a dirty insulator or encroaching vegetation. Monitoring such transient events provides an early opportunity to identify the trouble spot and take preventive measures.

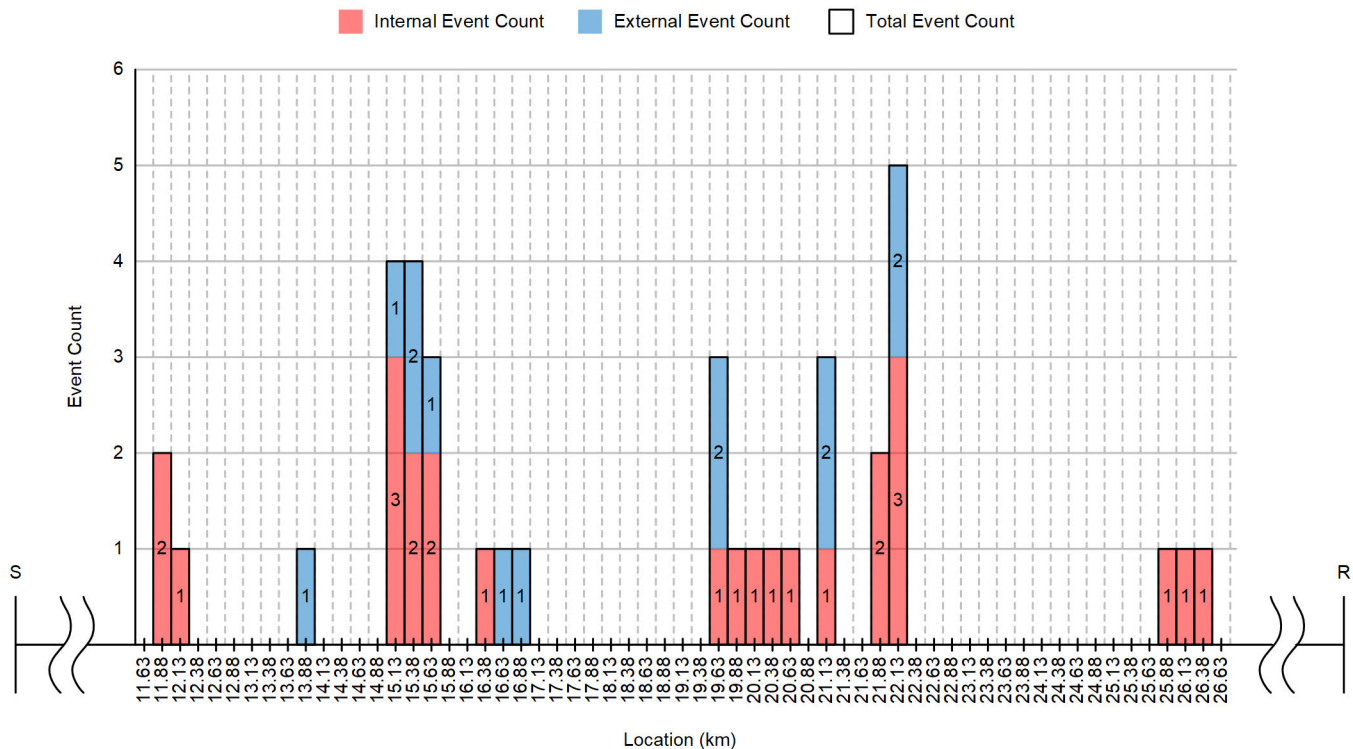


Fig. 22. Summary of event locations calculated from Terminal S for transient events recorded in a 30-minute interval prior to the fault (x-axis is zoomed in to show the event locations between 11 km and 27 km)

## VI. CONCLUSION

In this paper, we discuss the UHS protection and TW-based fault-locating principles employed by time-domain relays. The double-ended TWFL method provides accurate fault location for hybrid line applications involving overhead line and underground cable sections and can be used to adaptively control the autoreclosing scheme. This paper presents details about a pilot installation and configuration of UHS relays for protection and fault locating. A line energization test was performed to determine the TW line propagation time for each section of the hybrid line. UHS relay protection and fault-locating performance was evaluated for two internal faults and an external fault. The two internal faults were on the overhead line section, and the adaptive autoreclosing control logic successfully allowed reclosing for these faults. The high-resolution event recording in the UHS relays provided valuable TW information that could be used for monitoring, inspection, and preventive system maintenance.

The UHS relays installed for this pilot project employ a line monitor feature that calculates, tabulates, and records event locations for any low-energy or high-energy event reported on a line. This feature provides real-time system monitoring. By capturing and reporting precursors to faults, the line monitor feature provides the means to raise an alarm in time to identify trouble spots before they develop into permanent faults on the line. This can help when conducting preventive maintenance to ensure line health.

## VII. ACKNOWLEDGMENT

The authors gratefully acknowledge the contribution and support of the utility's engineers and field crew on this pilot project.

## VIII. REFERENCES

- [1] E. O. Schweitzer, III, V. Skendzic, A. Guzmán, M. V. Mynam, J. L. Eternod, and Y. Gong, "Mystery Solved: Five Surprises Discovered With Megahertz Sampling and Traveling-Wave Data Analysis," proceedings of the 72nd Annual Conference for Protective Relay Engineers, College Station, TX, March 2019.
- [2] B. Kasztenny, A. Guzmán, M. V. Mynam, and T. Joshi, "Locating Faults Before the Breaker Opens – Adaptive Autoreclosing Based on the Location of the Fault," proceedings of the 44th Annual Western Protective Relay Conference, Spokane, WA, October 2017.
- [3] E. O. Schweitzer, III, B. Kasztenny, A. Guzmán, V. Skendzic, and M. V. Mynam, "Speed of Line Protection – Can We Break Free of Phasor Limitations?" proceedings of the 41st Annual Western Protective Relay Conference, Spokane, WA, October 2014.
- [4] A. Guzmán, M. V. Mynam, V. Skendzic, J. L. Eternod, and R. M. Morales, "Directional Elements – How Fast Can They Be?" proceedings of the 44th Annual Western Protective Relay Conference, Spokane, WA, October 2017.
- [5] E. O. Schweitzer, III, B. Kasztenny, and M. V. Mynam, "Performance of Time-Domain Line Protection Elements on Real-World Faults," proceedings of the 42nd Annual Western Protective Relay Conference, Spokane, WA, October 2015.
- [6] E. O. Schweitzer, III, "A Review of Impedance-Based Fault Locating Experience," proceedings of the Northwest Electric Light & Power Association Conference, Bellevue, WA, April 1988.

- [7] A. Guzmán, B. Kasztenny, Y. Tong, and M. V. Mynam, “Accurate and Economical Traveling-Wave Fault Locating Without Communications,” proceedings of the 44th Annual Western Protective Relay Conference, Spokane, WA, October 2017.
- [8] A. Greenwood, *Electrical Transients in Power Systems*, 2nd ed., Wiley Interscience, New York, NY, 1991.
- [9] E. O. Schweitzer, III, A. Guzmán, M. V. Mynam, V. Skendzic, B. Kasztenny, and S. Marx, “Locating Faults by the Traveling Waves They Launch,” proceedings of the 40th Annual Western Protective Relay Conference, Spokane, WA, October 2013.
- [10] J. L. Blackburn and T. J. Domin, *Protective Relaying Principles and Applications*, 4th ed., CRC Press, Boca Raton, FL, 2014.

## IX. BIOGRAPHIES

**Shitaprajnyan Sharma** received his post-graduate diploma in international business, with honors, from the Indian Institute of Foreign Trade in 2016 and his BE in electrical engineering, with honors, from Utkal University in 2006. He started his professional career with SPML as a power system design engineer. Later, he worked for ABB as a protection engineer. He joined Schweitzer Engineering Laboratories, Inc. in 2011 as an application engineer and is currently working as an application engineering manager in India. He has been involved in substation and generator protection, fast motor bus transfer solutions, application engineering, testing, and commissioning of protection and control solutions.

**Amol Kathe** received his bachelor’s degree in electrical engineering from Mumbai University in Mumbai, India, in 2006 and his master’s degree in electrical engineering from Michigan Technological University in Houghton, MI, in 2014. He worked for over five years as a manager at Reliance Infrastructure Limited in the operations department of the energy division. He joined Schweitzer Engineering Laboratories, Inc. in 2014 and holds the position of power engineer in the research and development division.

**Titiksha Joshi** is a power engineer in the research and development division at Schweitzer Engineering Laboratories, Inc. She received her bachelor’s degree in electrical engineering from Mumbai University, India, in 2012 and her Master of Science degree in electrical engineering from Arizona State University in 2014. She has worked as an intern at Crompton Greaves (2011) and Midcontinent Independent System Operator, Inc. (2013).

**Thamizhcholai Kanagasabai** received his bachelor’s degree in electrical and electronics engineering from Anna University, Chennai in 2010. He started his professional career with power system design and commissioning services as a protection engineer. He joined Schweitzer Engineering Laboratories, Inc. in 2016 and holds the position of application engineer.